

Effects of Confinement on the Self-Organization of Microtubules and Motors

M. Pinot,¹ F. Chesnel,² J.Z. Kubiak,² I. Arnal,³ F.J. Nedelec,⁴ and Z. Gueroui^{1,*}

¹Centre National de la Recherche Scientifique (CNRS)/University of Rennes 1

Institut de Physique de Rennes (IPR)

UMR 6251

35042 Rennes

France

²CNRS/University of Rennes 1

UMR 6061

35043 Rennes

France

³CNRS/University of Rennes 1

UMR 6026

35042 Rennes

France

⁴Cell Biology and Biophysics Unit

European Molecular Biology Laboratory

Heidelberg D-69117

Germany

Summary

The regulation of the cytoskeleton is essential for the proper organization and function of eukaryotic cells. For instance, radial arrays of microtubules (MTs), called asters, determine the intracellular localization of organelles [1, 2]. Asters can be generated through either MT organizing center (MTOC)-dependent regulation or self-organization processes [1, 3, 4]. In vivo, this occurs within the cell boundaries. How the properties of these boundaries affect MT organization is unknown. To approach this question, we studied the organization of microtubules inside droplets of eukaryotic cellular extracts with varying sizes and elastic properties. Our results show that the size of the droplet determined the final steady-state MT organization, which changed from symmetric asters to asymmetric semi-asters and, finally, to cortical bundles. A simple physical model recapitulated these results, identifying the main physical parameters of the transitions. The use of vesicles with more elastic boundaries resulted in very different morphologies of microtubule structures, such as asymmetrical semi-asters, “Y-branching” organizations, cortical-like bundles, “rackets,” and bundled organizations. Our results highlight the importance of taking into account the physical characteristics of the cellular confinement to understand the formation of cytoskeleton structures in vivo.

Results and Discussion

Asters can be produced through cross-linking and moving of microtubules (MTs) by oligomeric motors in vitro [3, 4]. Recent experiments suggest interplay between the cell shape and intracellular cytoskeleton organization [5–8]. Yet, the techniques

available for investigation of the effects of boundaries are still limited. In vivo studies rely mainly upon recent microfabrication advances that allow the design of microenvironments of well-defined geometrical and surface patterning [8–11]. In vitro experiments performed in microfabricated chambers showed the importance of forces produced by the polymerization of MTs on their three-dimensional organization or on self-centering of MTOCs [12–14].

Recently, the compartmentalization of biomolecules inside droplets has been successfully used for biochemical assays [15, 16] and for studying confined biopolymers [17–19]. Here, we extend the compartmentalization techniques to quantitatively examine the effects of size and elasticity of cell boundaries on the self-organization of MTs and motors. Femto-liters of eukaryotic cytoplasmic extracts were enclosed inside emulsion droplets (a droplet of extracts surrounded by oil) or inside vesicles. Although the boundary in both droplets and vesicles lacks the functionalities normally found in the cortex of cell membranes, this bottom-up strategy isolates some general physical principles and allows their quantitative study [20, 21].

Self-Organization of Microtubules and Motors inside Rigid Droplets

To investigate the effect of a confined environment on MT self-organization, we developed a method to generate droplets of *Xenopus laevis* egg extracts dispersed in oil. These metaphase II-arrested oocyte extracts contain all the components necessary for the formation of self-organized MT asters in metaphase [22, 23]. Fluorescently labeled tubulin was mixed with the egg extracts, allowing for observation of MT formation and organization via fluorescent microscopy. First, we analyzed the ability of MTs to form asters in nonconfined *Xenopus* cell extracts that were complemented with taxol for the enhancement of MT nucleation and stability. We observed that in this system, growing MTs were spontaneously organized into radial arrays, probably by minus-end-directed motors such as dyneins, which are known to be present in extracts [23] (Figures 1A and 1B). Extract-in-oil droplets with a diameter of 0.5 μm to 70 μm were formed within few seconds by the stirring of a mixture of cell extracts (3% v/v) and mineral oil. The extract was supplemented with fluorescently-labeled tubulin, which was initially homogeneous (Figure 1D). After 5 min of incubation, approximately 75% of the droplets contained visible micrometer-sized MT bundles (Figure 1E).

In nonconfined extracts, MTs assemble in asters reaching a steady-state diameter of $28 \pm 4 \mu\text{m}$ within 15 min (Figure S1A, available online). To test whether MTs behaved similarly in the confined extracts, we first analyzed droplets larger than 29 μm (average aster diameter) to avoid any perturbation due to the confinement. Our results show that in those droplets, MTs organized mostly in radial arrays similar to those observed in nonconfined extracts (Figures 2A and 2D). The distribution of fluorescence intensity of radial asters in droplets was similar to that seen in bulk measurements (Figure S1B). In addition, time-point measurements suggested that MTs organized in fully developed asters within 15 min for both unconfined and confined extracts (Figure S2B). This suggests that the components of the extracts behaved similarly in droplets and in bulk.

*Correspondence: zoher.gueroui@univ-rennes1.fr

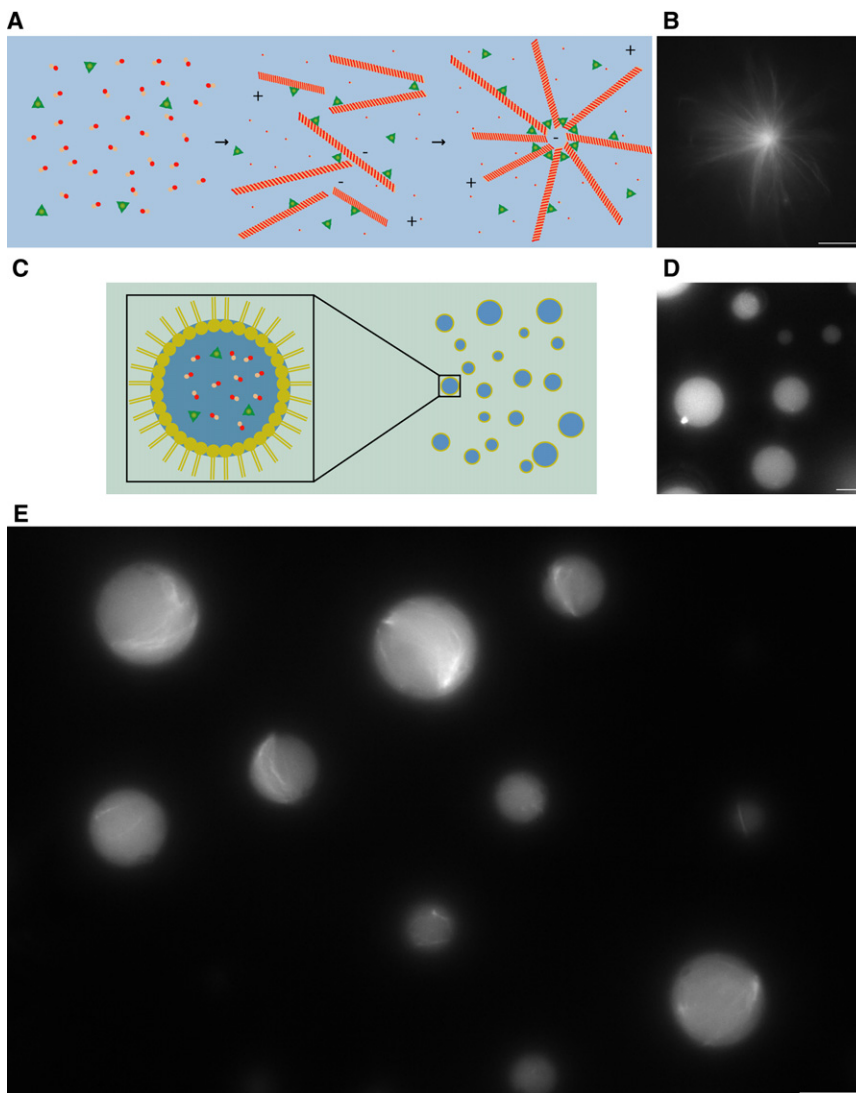


Figure 1. Self-Organization of Microtubules and Motors inside Droplets

(A) Schematic representation of aster self-organization in *Xenopus* egg extracts. Microtubules randomly grow throughout the cytoplasm and are organized by minus-end-directed motor proteins. Motor protein complexes cross-link neighboring filaments and organize them in radial arrays (green triangles: oligomeric motors; orange dots: tubulin dimers).

(B) Fluorescent observation of a fully developed aster in *Xenopus* egg extracts after a 10 min incubation.

(C) Schematic representation of the extract-in-oil droplet.

(D and E) Extract-in-oil droplets at the initial stage (D) and after a 10 min incubation (E). Scale bars represent 10 μm .

Figure S4E). These qualitative observations were confirmed by quantifying, for each diameter category, the percentage of droplets containing each of these three MT structures (Figure 2D). For each diameter category, more than 93% of the droplets contained MTs organized in the characteristic morphology. Coexistence of asters and semi-asters was observed within a narrow range of droplet size (26–30 μm ; Figure S3A). This coexistence might be the consequence of the intrinsic variability in aster assembly, as indicated, for instance, in the distribution of aster diameters (Figure S1A).

To determine whether the MT arrays are polarized within droplets, we used fluorescent stabilized MT seeds, which allowed us to distinguish the minus end of MT bundles from the plus end, given that assembly is faster at the growing

MT plus end. For semi-aster structures, seeds colocalized mainly at the poles, indicating their minus-end nature (Figure 2E). In addition, analysis of semi-aster pole orientation showed that the direction of the polarization is random in space (Figure 2F).

To investigate whether a motor activity is required in the MT organizing process, we added to the extract-in-oil droplets either p50/dynactin, which is a subunit of dynactin known to perturb the dynein-dynactin motor activity [24], or ortho-vanadate, which is an inhibitor of dynein ATPase activity. In these experimental conditions, MTs became organized mostly in randomly oriented bundles or cortically, rather than in asters or semi-asters (Figures S5A–S5H), showing the essential role of dynein-dynactin in assembling MTs into asters in our system.

Taken altogether, our results suggest that MT organization by minus-end motors can self-polarize, even in the absence of external cues or structural anisotropy of the environment, for a specific range of confinement size.

Physical Mechanisms Determine Microtubule Self-Organization under Confinement

What are the mechanisms determining MT organization and their transition as a function of the confinement size? We

Microtubule-Based Structures Undergo Symmetry Breaking as a Function of Droplet Size

Given the wide range of obtained droplet sizes, our system is ideal for examining the effect of variance in the diameter of a spherical confinement on MT self-organization. Indeed, because the surface tension between the oil and the extract is high, the confinement is always rigid and spherical (Figures 1C and 1D). We next analyzed MT organization with regard to the size of the droplets. Remarkably, we noticed three characteristic MT motifs, each associated with a specific range of droplet diameters. In droplets larger than 29 μm , MTs organized in asters that were centered within the droplet (Figure 2A and Figure S4A). For droplets between 11 and 29 μm , MTs organized mostly in asymmetrically focused structures (semi-asters) with their pole near the surface of the droplet (Figure 2B and Figures S4B and S4C). Time-series acquisitions illustrate MT organization and pole movement within a droplet (Figures S2B–S2E) and transition to asymmetric structures (Movies S1 and S2). Once MTs organized in asymmetric structures, their poles were dynamic, showing that they were not physically linked to the oil-extract interface (Movie S3). Finally, for droplet diameters ranging from 4 to 11 μm , microtubules were bent cortically (Figure 2C and

Confinement of Microtubules and Molecular Motors

3

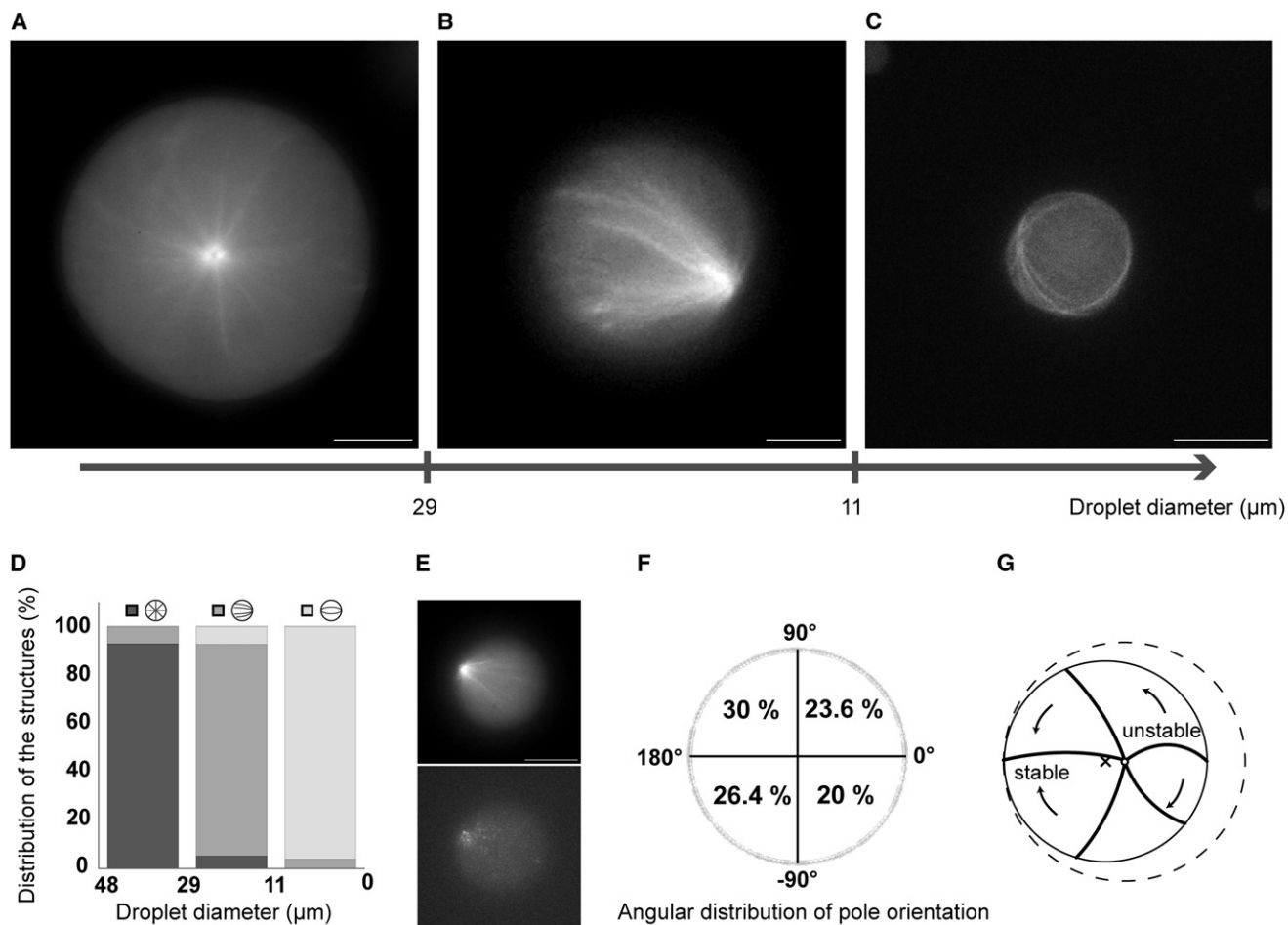


Figure 2. Microtubule-Based Structures Undergo Symmetry Breaking as a Function of Droplet Size

Fluorescent observations of microtubule structures inside droplets of different diameters.

(A) A radial aster inside a 39 μm droplet.

(B) An asymmetrical semi-aster inside a 25 μm droplet.

(C) A cortical-like configuration inside an 11 μm droplet.

(D) Proportions of radial asters, asymmetrical semi-asters, and cortical-like bundles as a function of the droplet size (600 droplets out of 21 experiments).

(E) Colocalization of MT bundles of a semi-aster (top) with fluorescent marker of MT polarity (bottom).

(F) Orientation of the poles of 385 semi-asters. The distribution is consistent with a random orientation. Scale bars represent 10 μm .

(G) The center of a sphere is an unstable position for a self-organized aster. This model shows that the aster pole moves away from the geometrical center of the confinement (cross) in order to allow most of the MT filaments to adopt a configuration that is the least compressed and bent. Indeed, the most favorable configuration for a rigid fiber is the one with minimal curvature, minimizing the filament elastic energy. In the case of a self-organized aster in a sphere, when the fibers are slightly longer than the sphere radius, the configuration can be predicted with simple arguments. Microtubules can pivot around the focal point of the aster, meaning that in the absence of friction, they will all rotate on one side and push the pivot even further off-center to allow for the most favorable configuration for minimization of the filament elastic energy. Thus, the center is an unstable position. Even if microtubules are initially equally distributed, an instability arises between the angular distribution of the microtubule and the position of the focus point. The dashed circle represents the space of minimum compression and curvature for MTs.

used physical and geometrical arguments to describe how the radius at which MT-based structures switch from one arrangement to another can be linked to the mechanical properties of MTs and of the boundary.

Our observations of small droplets showed that MTs do not deform the droplet boundary, in agreement with the high value of the extract-oil surface tension. When growing MTs encounter the rigid droplet boundary, they experience compressive forces exerted by the extract-oil interfacial tension [25]. When the MT length is larger than the droplet perimeter (in the micrometer range), the fibers buckle and circle along the spherical confinement to minimize their bending elastic energy (Figure 2C, Supplemental Discussion, and Figure S4E).

The transition from an isotropic aster to a semi-aster seems to be the point at which the diameter of the droplet is comparable to the diameter of the aster. Indeed, the transition size of 29 μm matches the size of asters formed in the absence of confinement (Figure 2D and Figure S1A). At this point, the geometric center of a growing aster becomes unstable. In general, predicting the configuration of a confined aster is quite complex. However, in Figure 2G we present a simple model explaining how a radial aster, having a diameter slightly larger than the confinement, becomes asymmetric. This model shows that the aster pole moves away from the geometrical center of the confinement in order to allow most of the MT filaments to adopt a configuration that is the least compressed and bent (Figure 2G).

The behavior of a self-organized aster described above is distinct from an aster generated by a MTOC confined in rigid boxes [12]. First, whereas in the experiments performed with MTOCs the MTs were confined in square boxes, our experiments were performed with MTs inside spherical droplets without corners. Second, MTs in self-organized asters are constrained in position but still have the capability to pivot around their minus-ends, whereas a MTOC additionally constrains MTs in a particular direction. This can explain why the self-organized semi-asters in our experiments were positioned at the vicinity of the physical boundary, whereas the most favorable position for the geometrical center of an MTOC aster is between the center of the chamber and its edge. Thus, the center of a sphere is an unstable position for a self-organized aster (see [Figure 2G](#)). In addition, directed movement of minus-end motors that can transport MTs amplifies any deviation from the geometrical center. Physically, the formation of semi-asters corresponds to a spontaneous symmetry-breaking event, which is expected to occur in a random direction ([Figure 2E](#)). This is analogous to the spontaneous cell polarization of the acto-myosin system in budding yeast, in which a built-in positive feedback is thought to amplify small stochastic variations in the concentration of polarity proteins [26, 27].

Numerical Simulations of Confined Microtubules and Motors

To determine whether a simple physical model could explain the observed transitions, we performed numerical simulations taking into account some of the known properties of MTs and motor proteins. MTs were modeled as semi-flexible polar polymers that all share the same fixed length. They were confined in two dimensions in a disc with frictionless boundaries and could be cross-linked by processive minus-end motors. Several parameters, including the bending elasticity of MTs, the concentration and properties of motors, and the size of the droplet, were considered in the simulation (see [Table S1](#)). We systematically examined the relationship between the confinement size, MT length, and organization and found that the computed configurations reproduced the patterns observed experimentally ([Figures 3A–3C](#)). For each case, we performed several runs of the simulation, all of which differed as a result of the stochastic nature of the model [28]. The transition between a radial array and a semi-aster occurred when the droplet diameter (29 μm) matched the aster length (29 μm). [Figure 4D](#) shows that the majority of the structures were radial at 30 μm and asymmetric at 27 μm when MT lengths were fixed to 29 μm , confirming the sharpness of the transition observed experimentally. The variability in the final organization of MTs under confinement arises mostly from the random initial configurations and the stochastic nature of motor activity ([Figure 3D](#) and [Figures S3](#) and [S3C](#)).

The transition between semi-asters and cortical arrangements occurred when individual MTs were long enough to buckle and circle along the contour of the compartment; this was observed for a confinement diameter of 10 to 13 μm ([Figure 3E](#)).

Numerical simulations were also used to investigate other parameters inaccessible in our experimental assay. We tested the condition in which MT rotation around the aster pole was constrained, which could mimic a rigid MTOC aster, and showed that in this case radial asters did not undergo the transition toward an asymmetric structure (see [Supplemental](#)

[Discussion](#) and [Figure S7D](#)). This suggests that the ability of MTs to pivot around their minus end is a key parameter of the symmetry-breaking process. We also tested the geometry of the confinement. Interestingly, simulations of self-organized asters confined in a square box showed that MTs and motors do not organize into an asymmetric structure, contrary to what is observed with a spherical confinement ([Supplemental Discussion](#) and [Figure S7F](#)). Thus, the confinement geometry plays a major role in self-organization of MTs and motors.

Numerical simulations thus succeed in reproducing both the final steady-state organization of MTs and the radius of transition observed experimentally. Taken altogether, our results confirm that the main parameters controlling transitions in MT and motor self-organization are the MT length and the confinement diameter.

Self-Organization of Microtubules and Motors Depends on Membrane Bending Stiffness

Whereas unicellular eukaryotes such as yeasts have rigid cell walls, many higher eukaryotic cells have a deformable cortex. To mimic this, we encapsulated the extracts in a lipid bilayer in a two-step process that allowed a precise control of the cytoplasm-encapsulation procedure ([Figure 4A](#)). In addition, with this method, we tuned the membrane bending stiffness from $k \sim 1\text{--}6 \times 10^{-19}$ J by changing the cholesterol content from 5% to 50% [29], thus increasing cohesion between adjacent lipids. As a result of this stiffness, MTs may deform the cell membrane, something that is impossible with extract-in-oil droplets ([Supplemental Discussion](#)).

Five minutes after the vesicles were generated, a limited number of morphologies of quasi-spherical shape was observed. Some of these structures also exhibited micrometer-sized membrane tubes containing MTs ([Figures 4B–4E](#)). The overall membrane shapes were classified as a function of the internal microtubule architectures in asymmetrical semi-asters, “Y-branching” organizations, cortical-like bundles, “rackets,” and linear bundles ([Figure 4F](#)). Interestingly, these morphologies depend not only on the confinement size but also on the bending stiffness of the membrane. For a bending stiffness of $k \sim 6 \times 10^{-19}$ J (50% cholesterol), 73% of vesicles were quasi-spherical, having either cortical-like bundles (diameter 4–10 μm ; [Figure 4C](#)) or semi-asters (12–16 μm ; [Figure 4D](#)). In contrast, for a bending stiffness of $k \sim 1 \times 10^{-19}$ J (5% cholesterol), 60% of the vesicles underwent important morphological changes associated with the formation of a single ([Figure 4B](#)) or multiple ([Figure S8](#)) MT-containing protrusions.

These morphological transformations were most likely determined by the membrane-rigidity- and force-generating elements, such as MTs [17], which drive filament sliding and overall structural rearrangement. For example, the morphological transition from a spherical vesicle to a vesicle with a single protrusion occurred when a critical force required for membrane buckling was reached; we estimate this as being between 25 and 45 pN ([Supplemental Discussion](#)).

Previous experiments explained different morphologies of vesicles deformed by microtubule growth by considering the elastic properties of the membrane [30, 31]. In our experiments, the presence of motors cross-linking several microtubule bundles led to the formation of various intracellular networks ([Figures 4D](#) and [4F](#)). Thus, the ability of intracellular organization to deform the membrane increased the number of possible morphological states, compared to those obtained within rigid droplets ([Figure 4F](#)).

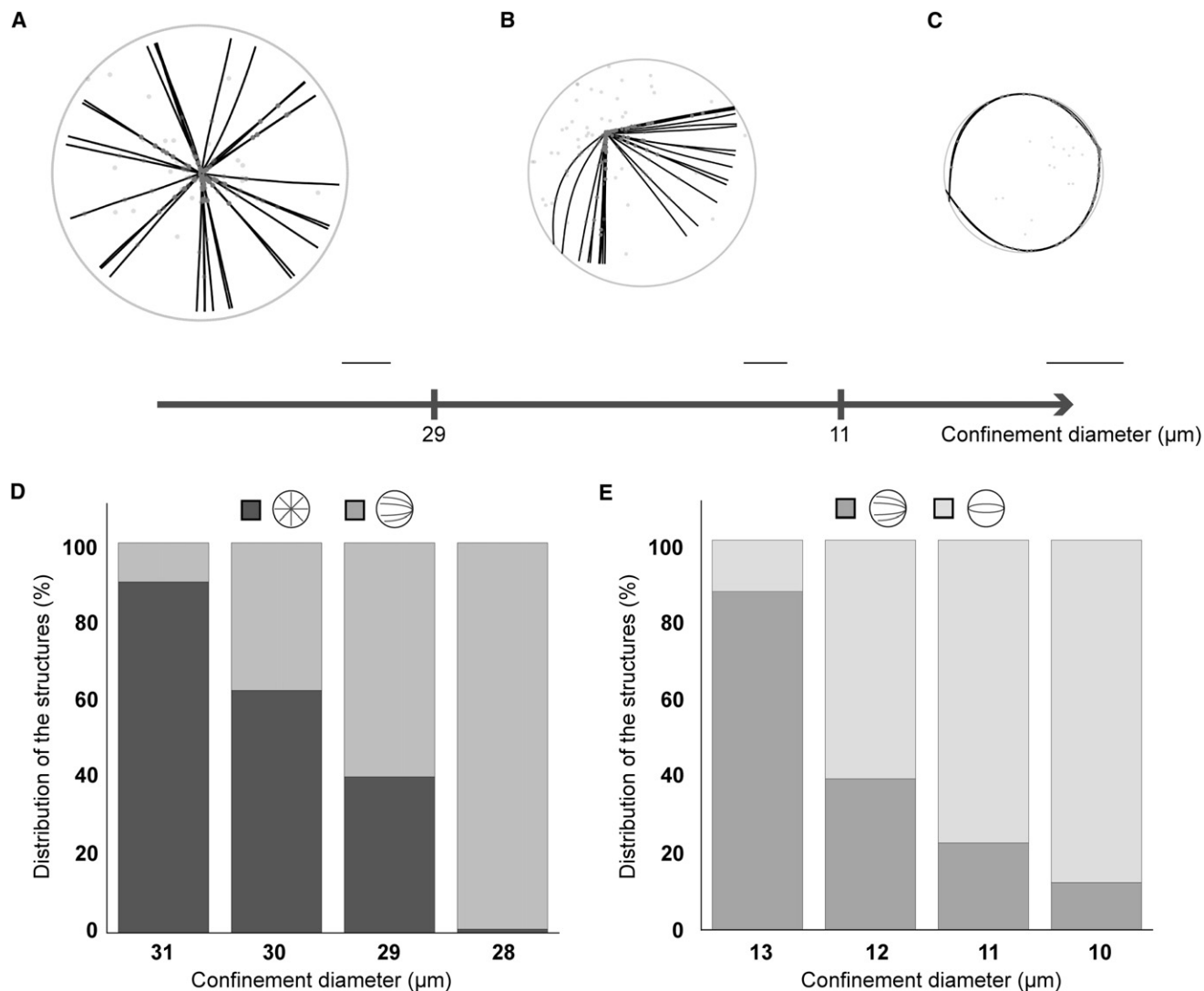


Figure 3. Examples of Computed Microtubule and Motor Protein Configurations as a Function of the Confinement Size

The parameters are set as in Table S1, unless otherwise specified. Microtubule length = 14.5 μm.

(A) Radial aster inside a 32 μm confinement (30 filaments, 1000 minus-end motor dimers [gray dots]).

(B) Asymmetrical semi-aster structure inside a 26 μm confinement (28 filaments, 1000 minus-end motor dimers).

(C) Cortical-like bundles inside a 10 μm confinement (six filaments, 500 minus-end motor dimers). Steady-state configurations of semi-asters obtained from numerical simulations showed a stochastic enrichment of motor complexes at the pole. This stochastic asymmetry is amplified by motor transport, a process faster than the Brownian diffusion of motors at the scale of the droplet.

(D and E) Distribution of the structures as a function of the confinement diameter (100 runs for each diameter). Scale bars represent 5 μm.

Conclusion

We found that symmetry breaking in MT organization arose for a specific range of confinement size, depending on the rigidity of the boundary. In particular, MT asters can self-polarize within a range of size in the absence of external cues. Softening the rigidity of the boundary led to different morphological states. The morphological transitions observed depend solely on MT length, confinement size, and membrane rigidity. Using a simple model, we showed that the physical characteristics of MTs and of boundaries are sufficient to explain the mechanism of the symmetry breaking observed. In particular, forces generated by MTs and minus-end motors drive filament sliding and overall structural rearrangement.

MT dynamic instability was reduced in our assay. We expect that in living cells, regulation of MT dynamic, by regulatory

proteins or MT force-dependent catastrophe, will allow the exploration of a larger number of morphological states [2, 32, 33].

In conclusion, the self-organization of MTs and motors is strongly affected by the presence of a boundary. Generic self-centering and self-polarizing regimes arise for different droplet sizes, showing the decisive influence of physical cell boundaries on internal MT organization. Our assay provides an easy bottom-up approach in which some general principles relating to the interplay between microtubule self-organized structures and cell shape can be illustrated. Living cells must accommodate these physical constraints. However, they use regulators, molecular motors, or other molecules in their membranes to further control their internal architecture. Functionalizing the boundaries of the droplets is therefore an exciting perspective for further study of the relationship between cytoskeleton organization and cell morphology.

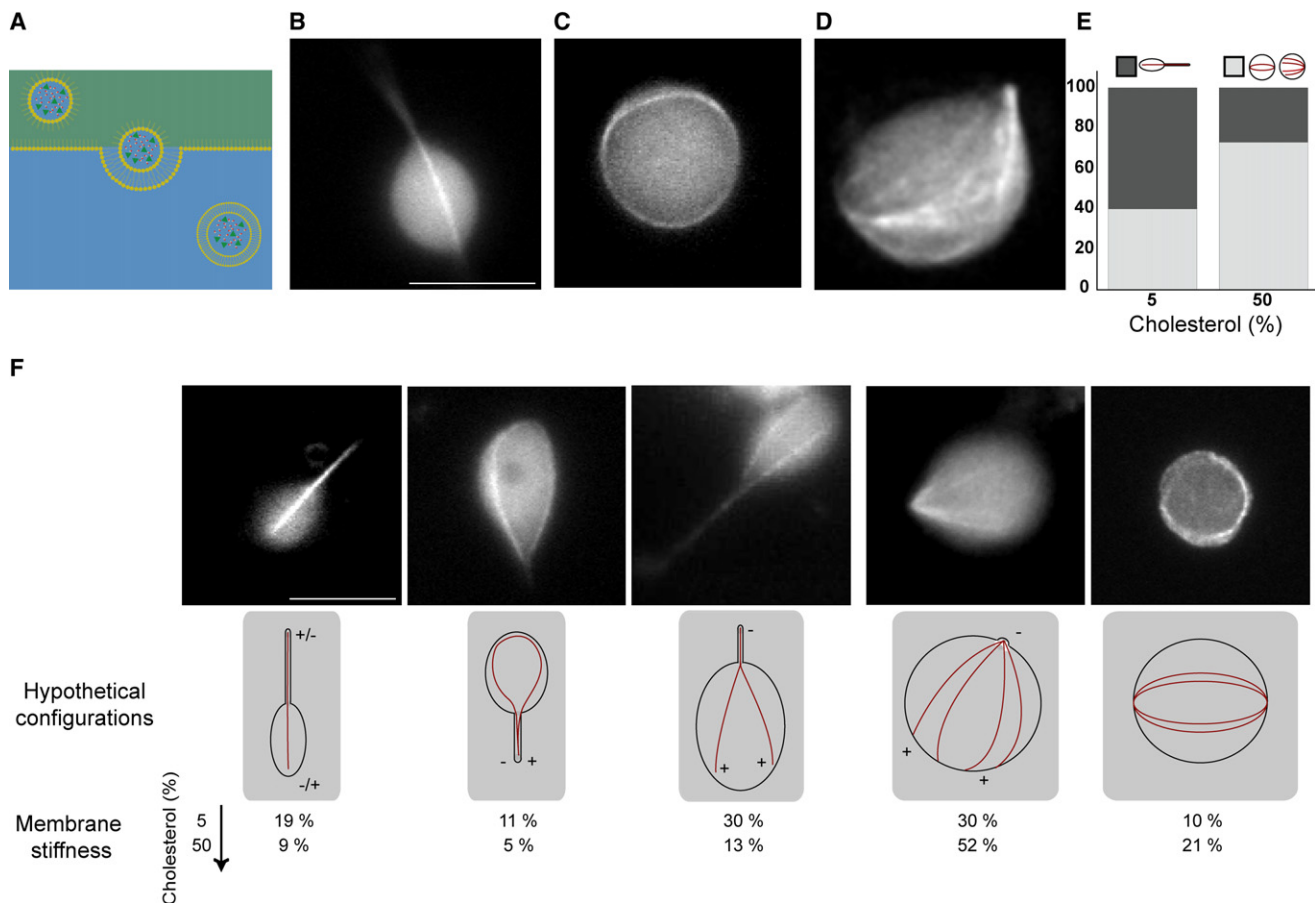


Figure 4. Self-Organization of Microtubules and Motors Depends on Membrane Bending Stiffness

(A) Schematic representation of the compartmentalization process of the *Xenopus* metaphase cell extract inside vesicles.

(B–D) Results of microtubule and motor self-organization inside vesicles formed with 5% or 50% cholesterol, corresponding to a membrane stiffness of roughly 1×10^{-19} J or 6×10^{-19} J, respectively.

(E) Percentage of morphologies as a function of the membrane stiffness.

(F) Fluorescence observations and schematic representations of microtubule-based structures inside vesicles as a function of the bending stiffness. Scale bars represent $10 \mu\text{m}$. Below the schematic representation, the percentage of vesicles containing each structure type is given for vesicles containing 5% cholesterol (top) or 50% cholesterol (bottom).

Supplemental Data

Supplemental Data include Supplemental Experimental Procedures, Supplemental Discussion, eight figures, two tables, and three movies and can be found with this article online at [http://www.cell.com/current-biology/supplemental/S0960-9822\(09\)01025-2](http://www.cell.com/current-biology/supplemental/S0960-9822(09)01025-2).

Acknowledgments

The authors wish to thank Albert Libchaber, Denis Chrétien, Anne Renault, and the IPR lab members for support and Pascal Panizza, Eric Karsenti, Franck Artzner, Frédéric Coquelle, Benjamin Vitre, and Fabrice Senger for helpful discussions and comments. We acknowledge the members of the Nedelec team involved in the development of Cytosim and the E.Karsenti lab for providing p50/dynamitin. This work was supported by the Agence Nationale de la Recherche (ANR) (JC05_440006), the Association pour la Recherche sur le Cancer (ARC) (4474), and the CNRS (to Z.G.), by the Volkswagen foundation (to F.J.N.), and by the ARC (4900) and the Ligue Contre le Cancer (to J.Z.K.). M.P. is a Ministère de la Recherche et des Nouvelles Technologies (MNRT) predoctoral fellow.

Received: November 24, 2008

Revised: April 8, 2009

Accepted: April 9, 2009

Published online: May 7, 2009

References

- Kirschner, M., and Mitchison, T. (1986). Beyond self-assembly: from microtubules to morphogenesis. *Cell* 45, 329–342.
- Kirschner, M., Gerhart, J., and Mitchison, T. (2000). Molecular “vitalism”. *Cell* 100, 79–88.
- Nedelec, F.J., Surrey, T., Maggs, A.C., and Leibler, S. (1997). Self-organization of microtubules and motors. *Nature* 389, 305–308.
- Surrey, T., Nedelec, F., Leibler, S., and Karsenti, E. (2001). Physical properties determining self-organization of motors and microtubules. *Nat. Cell Biol.* 292, 1167–1171.
- Carazo-Salas, R.E., and Nurse, P. (2006). Self-organization of interphase microtubule arrays in fission yeast. *Nat. Cell Biol.* 8, 1102–1107.
- Daga, R.R., Lee, K.G., Bratman, S., Salas-Pino, S., and Chang, F. (2006). Self-organization of microtubule bundles in anucleate fission yeast cells. *Cell Biol.* 8, 1108–1113.
- Haase, S.B., and Lew, D.J. (2007). Microtubule organization: cell shape is destiny. *Curr. Biol.* 17, R249–R251.
- Terenna, C.R., Makushok, T., Velve-Casquillas, G., Baigl, D., Chen, Y., Bornens, M., Paoletti, A., Piel, M., and Tran, P.T. (2008). Physical mechanisms redirecting cell polarity and cell shape in fission yeast. *Curr. Biol.* 18, 1748–1753.
- Romet-Lemonne, G., VanDuijn, M., and Dogterom, M. (2005). Three-dimensional control of protein patterning in microfabricated devices. *Nano Lett.* 5, 2350–2354.

Confinement of Microtubules and Molecular Motors

7

10. Whitesides, G.M., Ostuni, E., Takayama, S., Jiang, X., and Ingber, D.E. (2001). Soft lithography in biology and biochemistry. *Annu. Rev. Biomed. Eng.* 3, 335–373.
11. They, M., Racine, V., Pepin, A., Piel, M., Chen, Y., Sibarita, J.B., and Bornens, M. (2005). The extracellular matrix guides the orientation of the cell division axis. *Nat. Cell Biol.* 7, 947–953.
12. Holy, T.E., Dogterom, M., Yurke, B., and Leibler, S. (1997). Assembly and positioning of microtubule asters in microfabricated chambers. *Proc. Natl. Acad. Sci. USA* 94, 6228–6231.
13. Dogterom, M., Kerssemakers, J.W., Romet-Lemonne, G., and Janson, M.E. (2005). Force generation by dynamic microtubules. *Curr. Opin. Cell Biol.* 17, 67–74.
14. Cosentino Lagomarsino, M., Tanase, C., Vos, J.W., Emons, A.M., Mulder, B.M., and Dogterom, M. (2007). Microtubule organization in three-dimensional confined geometries: evaluating the role of elasticity through a combined in vitro and modeling approach. *Biophys. J.* 92, 1046–1057.
15. Griffiths, A.D., and Tawfik, D.S. (2006). Miniaturising the laboratory in emulsion droplets. *Trends Biotechnol.* 24, 395–402.
16. Noireaux, V., and Libchaber, A. (2004). A vesicle bioreactor as a step toward an artificial cell assembly. *Proc. Natl. Acad. Sci. USA* 101, 17669–17674.
17. Elbaum, M., Kuchnir Fygenon, D., and Libchaber, A. (1996). Buckling microtubules in vesicles. *Phys. Rev. Lett.* 76, 4078–4081.
18. Claessens, M.M., Bathe, M., Frey, E., and Bausch, A.R. (2006). Actin-binding proteins sensitively mediate F-actin bundle stiffness. *Nat. Mater.* 5, 748–753.
19. Limozin, L., and Sackmann, E. (2002). Polymorphism of cross-linked actin networks in giant vesicles. *Phys. Rev. Lett.* 89, 168103.
20. Karsenti, E. (2008). Self-organization in cell biology: a brief history. *Nat. Rev. Mol. Cell Biol.* 9, 255–262.
21. Carazo-Salas, R., and Nurse, P. (2007). Sorting out interphase microtubules. *Mol. Syst Biol.* 3, 95.
22. Desai, A., Murray, A., Mitchison, T.J., and Walczak, C.E. (1999). The use of *Xenopus* egg extracts to study mitotic spindle assembly and function in vitro. *Methods Cell Biol.* 61, 385–412.
23. Verde, F., Berrez, J.M., Antony, C., and Karsenti, E. (1991). Taxol-induced microtubule asters in mitotic extracts of *Xenopus* eggs: requirement for phosphorylated factors and cytoplasmic dynein. *J. Cell Biol.* 112, 1177–1187.
24. Wittmann, T., and Hyman, T. (1999). Recombinant p50/dynamitin as a tool to examine the role of dynactin in intracellular processes. *Methods Cell Biol.* 61, 137–143.
25. Cohen, A.E., and Mahadevan, L. (2003). Kinks, rings, and rackets in filamentous structures. *Proc. Natl. Acad. Sci. USA* 100, 12141–12146.
26. Wedlich-Soldner, R., and Li, R. (2003). Spontaneous cell polarization: undermining determinism. *Nat. Cell Biol.* 5, 267–270.
27. Wedlich-Soldner, R., Altschuler, S., Wu, L., and Li, R. (2003). Spontaneous cell polarization through actomyosin-based delivery of the Cdc42 GTPase. *Science* 299, 1231–1235.
28. Nedelec, F., and Foethke, D. (2007). Collective Langevin dynamics of flexible cytoskeletal fibers. *New J. Phys.* 9, 24.
29. Meleard, P., Gerbeaud, C., Pott, T., Fernandez-Puente, L., Bivas, I., Mitov, M.D., Dufourcq, J., and Bothorel, P. (1997). Bending elasticities of model membranes: influences of temperature and sterol content. *Biophys. J.* 72, 2616–2629.
30. Fygenon, D.K., Marko, J.F., and Libchaber, A. (1997). Mechanics of Microtubule-Based Membrane Extension. *Phys. Rev. Lett.* 79, 4497.
31. Emsellem, V., Cardoso, O., and Tabeling, P. (1998). Vesicle deformation by microtubules: A phase diagram. *Physical Review E* 58, 4807–4810.
32. Janson, M.E., de Dood, M.E., and Dogterom, M. (2003). Dynamic instability of microtubules is regulated by force. *J. Cell Biol.* 161, 1029–1034.
33. Gregoret, I.V., Margolin, G., Alber, M.S., and Goodson, H.V. (2006). Insights into cytoskeletal behavior from computational modeling of dynamic microtubules in a cell-like environment. *J. Cell Sci.* 119, 4781–4788.